Original Paper

Caries Research

Caries Res 2014;48:73–89
DOI: 10.1159/000354123

Received: May 2, 2013
Accepted after revision: June 28, 2013
Published online: November 14, 2013

Numerical Modelling of Tooth Enamel Subsurface Lesion Formation Induced by Dental Plaque

O. Ilie[a] A.G. van Turnhout[b] M.C.M. van Loosdrecht[a] C. Picioreanu[a]

Departments of [a]Biotechnology and [b]Geoscience and Engineering, Delft University of Technology, Delft, The Netherlands

Key Words
Demineralisation · Enamel · Fluoride · Mathematical model · Oral biofilms · Subsurface lesion

Abstract
Using a one-dimensional mathematical model that couples tooth demineralisation and remineralisation with metabolic processes occurring in the dental plaque, two mechanisms for subsurface lesion formation were evaluated. It was found that a subsurface lesion can develop only as the result of alternating periods of demineralisation (acid attack during sugar consumption) and remineralisation (resting period) in tooth enamel with uniform mineral composition. It was also shown that a minimum plaque thickness that can induce an enamel lesion exists. The subsurface lesion formation can also be explained by assuming the existence of a fluoride-containing layer at the tooth surface that decreases enamel solubility. A nearly constant thickness of the surface layer was obtained with both proposed mechanisms. Sensitivity analysis showed that surface layer formation is strongly dependent on the length of remineralisation and demineralisation cycles. The restoration period is very important and the numerical simulations support the observation that often consumption of sugars is a key factor in caries formation. The calculated profiles of mineral content in enamel are similar to those observed experimentally. Most probably, both studied mechanisms interact in vivo in the process of caries development, but the simplest explanation for subsurface lesion formation remains the alternation between demineralisation and remineralisation cycles without any pre-imposed gradients.

Dental caries usually starts with a lesion in the superficial enamel layer (i.e., initial caries) developing under the influence of dental plaque metabolism. If the process is not stopped, such a lesion will advance until the dentino-enamel junction and even beyond, into the dentin and pulp. The study of the initial stages of caries development is important in understanding the disease as a whole, but also in coming up with restorative strategies since in the early stages the process is reversible [Fejerskov and Kidd, 2008]. One aspect that is not well understood currently concerns the aspect of initial lesions. The typical mineral profile of initial dental caries shows a region of roughly 100 μm at the tooth surface seemingly unaffected by demineralisation [Fejerskov and Kidd, 2008], with the main body of the lesion present under this surface layer. The differences in mineral content between the two zones can become considerable, especially in the more advanced

KARGER

E-Mail karger@karger.com
www.karger.com/cre

0008–6568/14/0481–0073$39.50/0

Olga Ilie
Department of Biotechnology, Delft University of Technology
Julianalaan 67
NL–2628 BC Delft (The Netherlands)
E-Mail o.ilie@tudelft.nl

stages of caries development: up to 99% mineral content in the surface layer compared to just 50–75% in the body of the lesion [Robinson et al., 2000; Fejerskov and Kidd, 2008]. This particular profile has been observed for the first time by Hollander and Saper [1935], who mistook it for a photographic artefact. Since then, much research – both experimental and theoretical – has been carried out in order to confirm and explain the phenomena responsible for subsurface lesion formation [Gray and Francis, 1963; Van Dijk et al., 1979; Langdon et al., 1980; Ten Cate, 1983; Margolis and Moreno, 1985].

From the hypotheses made to explain the mechanisms behind surface layer formation, two have received special attention. These hypotheses have been tested in the current study.

(1) Initial dental caries is mainly the consequence of an imbalance between two concurrent processes, demineralisation and remineralisation of tooth enamel [Loesche, 1986; Hicks et al., 2004; Fejerskov and Kidd, 2008]. These processes have the same thermodynamic driving force and can both occur in vivo. Therefore, the formation of a surface layer covering a subsurface lesion is seen as the result of an imbalance following repeated cycles of demineralisation (during meals) and remineralisation (between meals).

(2) The mineral crystals are less soluble at the enamel surface. This might be due to the following: (i) A fluoride distribution in the enamel depth with the highest content at the surface [Arends and Christoffersen, 1986; Fejerskov and Kidd, 2008]. The fluoride is incorporated into a hydroxyapatite (HAP) structure forming a more stable mineral, fluorohydroxyapatite (FHAP), which makes the enamel less soluble during acid attacks [Koutsoukos et al., 1980; Robinson et al., 2000]. (ii) HAP crystals with higher purity (hence, lower solubility) may develop at the enamel surface through a process called 'Ostwald ripening' [Robinson et al., 2000; Fejerskov and Kidd, 2008].

Other hypotheses in the dentistry literature have been proposed to explain the surface layer: faster remineralisation and delayed diffusion at the tooth surface [Silverstone, 1977; White et al., 1988], presence of chemical species that inhibit subsurface remineralisation [White et al., 1988], presence of salivary proteins that inhibit surface demineralisation and remineralisation [White et al., 1988], and phase transformation at the tooth surface resulting in the formation of dicalcium phosphate dehydrate [Margolis and Moreno, 1985; Fejerskov and Kidd, 2008]. Although plausible, some of these premises are too speculative or cannot alone explain the formation of the surface layer.

The interaction between physical, chemical and (micro)biological aspects involved in subsurface lesion formation is highly complex. Intuition and simple calculations may not be sufficient to allow a thorough theoretical evaluation of a conceptual hypothesis. Therefore, a series of numerical models of caries formation have been developed [Zimmerman, 1966a–c; Holly and Gray, 1968; Van Dijk, 1978; Ten Cate, 1983; Arends and Christoffersen, 1986]. These models could test with minimum effort hypotheses for which laborious experiments (some even impossible) would have been required. A disadvantage though is that all these models are simplified to deal exclusively with the processes occurring in the superficial layer of the tooth (demineralisation or remineralisation), without considering the active influence of the dental plaque. Moreover, demineralisation and remineralisation were not studied together, most of the models focusing on demineralisation only, with only few [Ten Cate, 1983, 2008] investigating tooth remineralisation.

The current work presents a one-dimensional, time-dependent mathematical model that integrates the kinetics of tooth demineralisation and remineralisation with mass transfer and with microbial conversions occurring in the dental plaque. The study is based on a previously developed numerical model for tooth demineralisation under the influence of an oral biofilm [Ilie et al., 2012], extended to evaluate the two main hypotheses for subsurface lesion formation. Our purpose was to establish which of the two theories can best explain the formation of a surface layer with the simplest assumptions. Case 1 assumes the tooth enamel is formed by HAP only and both demineralisation and remineralisation processes can occur, depending on the degree of saturation. Case 2 assumes that the tooth enamel includes FHAP crystals and studies the surface layer formation in the presence of a solubility gradient when only tooth demineralisation occurs.

Model Description

The one-dimensional numerical model for calculation of pH and solute concentrations in active dental plaque [Ilie et al., 2012] was extended to describe the subsurface lesion formation in the tooth enamel. In the present model, the dental plaque composition was simplified to only one generic microbial group with one fermentative pathway, in order to allow an increased complexity of tooth chemistry (while maintaining a reasonable computational effort).

Table 1. Model parameters

Parameter	Symbol	Value	Reference
Biomass concentration in plaque	C_X	100 g l^{-1}	Morgenroth et al., 2000
Maximum specific uptake rate	$q_{S,max}$	9.67×10^{-6} mol g^{-1} s^{-1}	van der Hoeven et al., 1985
Monod half-saturation coefficient for glucose	$K_{S,Glu}$	1.22×10^{-4} mol l^{-1}	Hamilton and St Martin, 1982 van der Hoeven et al., 1985
Proton inhibition constant	K_{I,H^+}	10^{-6} mol l^{-1}	assumed for inhibition at pH 4.5
Rate coefficients for dissociation equilibria	k_{LacH} k_{Pho^-}	10^6 s^{-1}	assumed[a]
Acidity constant for lactic acid	K_{LacH}	$10^{-3.86}$ mol l^{-1}	Atkins and De Paula, 2009
Acidity constant for dihydrogen phosphate dissociation	K_{Pho^-}	$10^{-7.21}$ mol l^{-1}	Atkins and De Paula, 2009
Acidity constant for hydrogen phosphate dissociation	$K_{Pho^{2+}}$	$10^{-12.32}$ mol l^{-1}	Atkins and De Paula, 2009
Acidity constant for water dissociation	K_{H_2O}	10^{-14} mol^2 l^{-2}	Atkins and De Paula, 2009
Enamel solubility constant	$K_{S,HAP(en)}$	7.41×10^{-60} mol^9 l^{-9}	Fejerskov and Kidd, 2008
HAP solubility constant	$K_{S,HAP}$	5.50×10^{-55} mol^9 l^{-9}	Fejerskov and Kidd, 2008
HAP molar weight	M_{HAP}	502 g mol^{-1}	Fejerskov and Kidd, 2008
HAP density	ρ_{HAP}	3,160 kg m^{-3}	Fejerskov and Kidd, 2008
Radius of HAP rod	r_{rod}	2.5×10^{-8} m	Fejerskov and Kidd, 2008
Demineralisation rate constant	k_d	7×10^{-6} $mol^{0.7}$ $m^{-1.1}$ s^{-1}	Margolis and Moreno, 1992
Remineralisation rate constant	k_r	7.44×10^{-3} $mol^{0.25}$ $m^{0.75}$ s^{-1}	Nancollas, 1983
Demineralisation reaction order	n_d	0.3	Margolis and Moreno, 1992
Demineralisation reaction order	m_d	2.8	Margolis and Moreno, 1992
Remineralisation reaction order	n_r	1.25	Nancollas, 1983
Length of tooth domain	L_t	100 µm	assumed
Length of dental plaque domain	L_p	250 µm	assumed[b]
Reduction factor for diffusion coefficients in the plaque	f_p	0.25	Dibdin, 1981
Time for the transition from $C_{Glu,min}$ to $C_{Glu,max}$	t_{step}	10 s	assumed
Feeding period	t_{feed}	2 min	assumed
Length of feeding/resting cycle	t_{cycle}	90 min	assumed
Halving time in the saliva film	$t_{h,f}$	0.5 min	Dibdin, 1990
Halving time in the saliva bulk	$t_{h,s}$	2.17 min	Dibdin, 1990
Residence time in the saliva film	Q_f/V_f	$\ln(2)/t_{h,f}$ min	calculated
Residence time in the saliva bulk	Q/V_s	$\ln(2)/t_{h,s}$ min	calculated
Area per volume ratio in saliva film	A_f/V_f	10^3 m^{-1}	calculated[c]
Minimum glucose concentration (between meals)	$C_{Glu,min}$	0.07 mM	Van der Hoeven et al., 1990
Maximum glucose concentration (during pulse)	$C_{S,Glu,max}$	560 mM	Dirksen et al., 1962
Universal gas constant	R	8.314 J mol^{-1} K^{-1}	–
Temperature	T	310 K	chosen, 37° C
Faraday's constant	F	96,485 C mol^{-1}	–

[a] Assumed an arbitrarily high value for very fast equilibria. [b] Based on the measured thickness of a 96-hour dental plaque, grown in vivo [Wood et al., 2000]. [c] Assumes that the saliva film thickness is 100 µm [Fejerskov and Kidd, 2008] and that only 10% of the tooth is covered with plaque.

Processes

Microbial Reactions

From the multitude of microbial processes occurring in dental plaque, only lactic fermentation was considered since it has the highest impact on caries formation [Dawes and Dibdin, 1986; Ilie et al., 2012]. This simplification still offers a good description of acidity production due to microbial metabolism, while allowing to focus the study on the porosity profile developed in the tooth. Consequently, the dental plaque was reduced to one microbial group, the aciduric *Streptococci*, with a constant concentration C_X in the plaque (i.e., no microbial growth was considered). This microbial group is commonly associated with caries development due to its high acidogenicity and aciduricity [Loesche, 1986; Marsh et al., 2009].

The anaerobic fermentation at high glucose concentration (equation 1) is the main source of lactic acid dur-

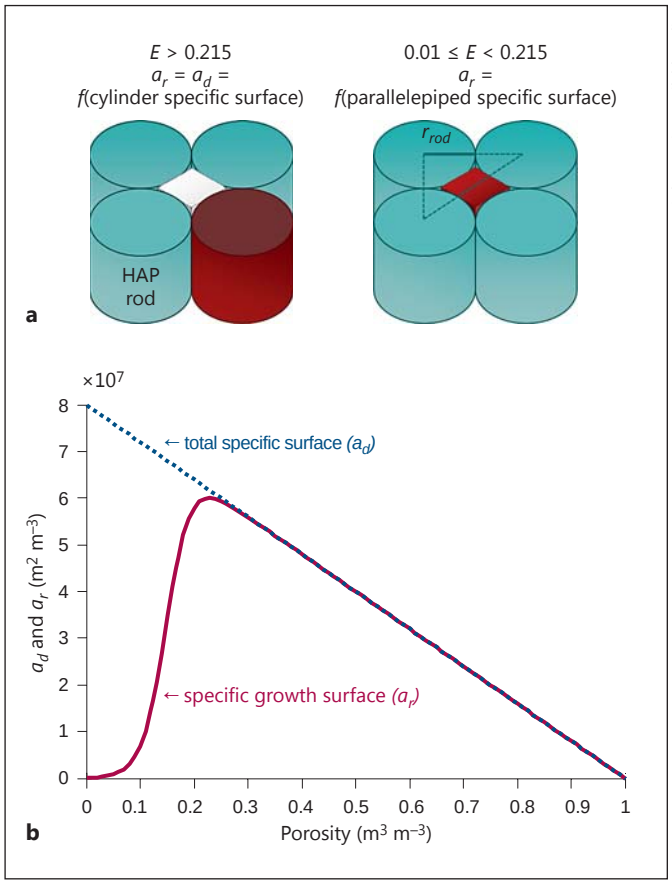

Fig. 1. a Schematic representation of the volume inside the tooth enamel. The HAP rods are assumed cylinders with a radius r_{rod}, while the inter-rod space is a parallelepiped. Left: calculation of the specific surface for remineralisation (a_r) at high enamel porosity function of area of the HAP cylinders. Right: low enamel porosity function of the inter-rod surface area. **b** Calculated total specific surface, a_d, and specific growth surface, a_r, function of enamel porosity E.

ing a cariogenic attack. Moreover, lactic acid is the strongest and most abundant acid present in fermenting dental plaque [Borgström et al., 2000].

$$C_6H_{12}O_6 \rightarrow 2C_3H_5O_3^- + 2H^+$$
$$r_{Glu} = q_{S,max}\, C_X \frac{C_{Glu}}{C_{Glu} + K_{S,Glu}} \frac{K_{I,H^+}}{C_{H^+} + K_{I,H^+}} \quad (1)$$

For the glucose uptake rate r_{Glu} (mol l^{-1} s^{-1}), Monod kinetics with glucose limitation (concentration C_{Glu}) and acid inhibition (proton concentration C_{H^+}) was assumed, with rate parameters given in table 1 [Van Beelen et al., 1986].

Acid-Base Equilibria

The simplified model includes very fast protonation equilibria for lactate (microbial metabolic product) and hydrogen phosphate (tooth demineralisation product) in all model compartments (saliva, plaque and tooth) (equations 2 and 3), with parameters in table 1:

$$C_3H_6O_3 \rightleftarrows C_3H_5O_3^- + H^+ \quad r_{LacH} = k_{LacH}\left(C_{LacH}\, K_{LacH} - C_{H^+}\, C_{Lac^-}\right) \quad (2)$$

$$H_2PO_4^- \rightleftarrows HPO_4^{2-} + H^+ \quad r_{Pho^-} = k_{Pho^-}\left(C_{Pho^-}\, K_{Pho^-} - C_{H^+}\, C_{Pho^{2-}}\right) \quad (3)$$

The other two phosphate equilibria were not considered because they only become important at pH values not reached in the current conditions. Although present in the previous dental plaque model, other possible inorganic buffers (e.g., CO_2/HCO_3^-) as well as complexation equilibria with Ca^{2+} and microbial surface charges were neglected here to simplify the analysis of results.

Tooth Demineralisation and Remineralisation

Following an analysis of mechanisms suggested in the literature for the formation of subsurface enamel lesions, two theories have been studied: case 1 – an alternation of two competing processes, enamel demineralisation and remineralisation, assuming only HAP crystals; case 2 – demineralisation of the tooth enamel composed of FHAP with higher concentration of fluoride at the enamel surface slowing down the dissolution rate. The model was adapted to each case, by considering different chemical reactions to occur in the tooth domain in addition to the acid-base equilibria.

It was assumed that the tooth enamel consists of parallel rods (represented as cylindrical crystals) of HAP, the spaces between them being filled with aqueous solution [Ten Cate, 1979]. Enamel porosity is the total volume of inter-rod spaces divided by total volume of the enamel (fig. 1a). Enamel porosity E is further used to characterize a lesion by the mineral content profile (i.e., the variation of (1 – E) over the first micrometres of enamel) and the lesion severity (i.e., the maximum porosity E reached within the lesion).

Case 1: Tooth Enamel Consisting of HAP

The first hypothesis is that the subsurface lesion is formed as a consequence of an imbalance between two concurrent processes, demineralisation and remineralisation. It was assumed that the tooth enamel consists of homogeneous HAP, therefore removing the bias of a solubility gradient due to, for example, a fluoride distribu-

Table 2. Chemical components in the model

Name	Symbol	Diffusion coefficient in water[c]		Saliva concentrations		
		(10^{-9} m^2 s^{-1})	reference	initial[a] $C_{f,j}(0)$, mol m^{-3}	inlet[b], mol m^{-3}	reference
Lactate ion	Lac^-	1.31	Vanýsek, 2001	0	0	assumed
Lactic acid	LacH	1.31	Vanýsek, 2001	0	0	assumed
Proton	H^+	11.81	Vanýsek, 2001	1.29×10^{-4}	8.71×10^{-4}	Fejerskov and Kidd, 2008
Hydrogen phosphate	Pho^{2-}	0.96	Vanýsek, 2001	4.27	2.24	equilibrium, $C_{Pho,tot\ initial}$ = 13.2 mol m^{-3} $C_{Pho,tot\ inlet}$ = 5.4 mol m^{-3}
Dihydrogen phosphate	Pho^-	1.22	Vanýsek, 2001	8.93	3.16	Fejerskov and Kidd, 2008 equilibrium
Calcium ion	Ca^{2+}	1.00	Vanýsek, 2001	3.5	1.32	Fejerskov and Kidd, 2008
Cation (potassium ion)	K^+	2.49	Vanýsek, 2001	51.5	19.4	Fejerskov and Kidd, 2008
Anion (chloride ion)	Cl^-	2.57	Vanýsek, 2001	41.03	14.4	charge balance
Fluoride ion	F^-	1.48	Vanýsek, 2001	6	1	Fejerskov and Kidd, 2008
Glucose	Glu	0.85	Vanýsek, 2001	0.07	$C_{s,Glu}(t)$	Van der Hoeven and Gottschal, 1989; calculated for inlet

[a] Values corresponding to those measured in human resting plaque (assumed to be in a steady state). [b] Values corresponding to those measured in unstimulated mixed (from all salivary glands) human saliva. [c] Diffusion coefficients for all solutes in water are reduced in plaque by a factor of 0.25 [Dibdin, 1981] and in the enamel reduced by the porosity E.

tion over the enamel depth. All the chemical species listed in table 2, with the exception of fluoride, have been included in this case.

For the HAP demineralisation reaction (equation 4)

$$Ca_5(PO_4)_3(OH) \leftrightarrows 5Ca^{2+} + 3PO_4^{3-} + HO^- \quad (4)$$

the empirical equation for the surface-based demineralisation rate, $r^*_{d,Ca}$ (mol Ca m^{-2} s^{-1}), was proposed in Margolis and Moreno [1992] (equations 5 and 6) (table 1).

$$r^*_{d,Ca} = k_d \left(1 - DS_{HAP}\right)^{m_d} \left(\sum C_{A(i)H}\right)^{n_d} \quad \text{for } DS_{HAP}<1 \quad (5)$$

$$r^*_{r,Ca} = 0 \quad \text{for } DS_{HAP} \geq 1 \quad (6)$$

The demineralisation rate is a function of the concentration of all protonated acids, $C_{A(i)H}$, and the degree of saturation of the solution with respect to HAP, DS_{HAP} (equation 7):

$$DS_{HAP} = \left(\frac{IP_{HAP}}{K_{S,HAP(en)}}\right)^{1/9} \quad \text{and}$$

$$IP_{HAP} = \frac{C^5_{Ca^{2+}}\, C^3_{Pho^{3-}}}{C_{HO^-}} = \frac{C^5_{Ca^{2+}}\, C^3_{Pho^{2-}}}{C^4_{H^+}}\, K^3_{Pho^{2-}}\, K_{H_2O} \quad (7)$$

DS_{HAP} depends on the ionic product IP_{HAP}, and the solubility constant, $K_{S,HAP(en)}$. Due to the impurities present in the tooth, the enamel solubility $K_{S,HAP(en)}$ has a lower value than that of pure HAP (table 1). The demineralisation occurs only when the solution is undersaturated in respect to HAP, DS_{HAP} <1.

The volumetric demineralisation rate of HAP (equation 8), $r_{d,HAP}$ (mol HAP m^{-3} s^{-1}), was derived by multiplying the surface-based rate with the specific crystal surface, a_d (m^2 m^{-3}), and considering the reaction stoichiometry (equation 4):

$$r_{d,HAP} = 0.2 r^*_{d,Ca}\, a_d \quad (8)$$

The specific crystal surface a_d was calculated as the area/volume ratio of a rod with a constant radius, r_{rod}, multiplied with the volume fraction of crystal in the enamel (the mineral content, 1 – E) [Ten Cate, 1979] (equation 9 and fig. 1b):

$$a_d = \frac{2}{r_{rod}}\left(1 - E\right) \quad (9)$$

The surface-based relation for HAP remineralisation rate, $r^*_{r,HAP}$ (mol HAP m^{-2} s^{-1}) (equations 10 and 11) was empirically determined by Nancollas [1983] from in vitro experiments on crystallisation of bovine enamel blocks.

$$r^*_{r,HAP} = k_r \left(DS_{HAP} - 1\right)^{n_r} \quad \text{for } DS_{HAP} \geq 1 \quad (10)$$

$$r^*_{r,HAP} = 0 \quad \text{for } DS_{HAP} < 1 \quad (11)$$

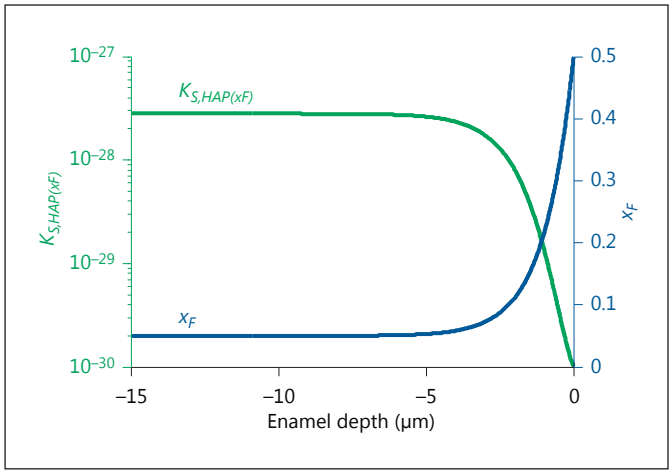

Fig. 2. Imposed distribution of fluoride fraction x_F and the mixed FHAP/HAP crystal solubility constant $K_{S,FHAP(xF)}$ within 15 μm from the enamel surface.

The lumped remineralization rate constant, k_r, and the reaction order, n_r, were calculated from the results of Nancollas [1983] (values in table 1).

The volumetric remineralisation rate, $r_{r,HAP}$ (mol HAP m^{-3} s^{-1}), was obtained from the surface-based rate multiplied with the specific growth surface, a_r (equation 12):

$$r_{r,HAP} = r^*_{r,HAP}\, a_r \tag{12}$$

The specific growth surface, a_r, is the fraction of the total specific surface, a_d, that is available for crystal growth (fig. 1a). Depending on the enamel porosity values *(E)*, the specific growth surface is calculated in two ranges:

(i) At porosity higher than 0.215 (corresponding to perfectly cylindrical HAP rods) [Ten Cate, 1979], the entire crystal surface is available for remineralisation (equation 13).

$$a_r = a_d = \frac{2}{r_{rod}}\left(1 - E\right), \text{ when } E > 0.215 \tag{13}$$

(ii) At porosity values lower than 0.215, as the inter-rod space gets filled, it was assumed that only a part of the total specific crystal surface a_d remains available for crystal growth. The a_r area was assumed to become zero when porosity reaches a minimal value E_{min} (i.e., remineralisation stops when $E_{min} = 0.01$). No pre-existing gradients in porosity were assumed and a uniform initial porosity E_{min} for healthy enamel was considered [Fejerskov and Kidd, 2008]. The specific growth surface was in this case calculated from a sigmoid function making the growth-specific area zero at E_{min}, mimicking a shrinking parallelepiped inter-rod space (fig. 1b) (equation 14).

$$a_r = a_d\left(1 - \frac{1}{1 + \exp\left(45\left(E - 0.15\right)\right)}\right), \text{ when } 0.01 < E < 0.215 \tag{14}$$

Finally, the change in enamel porosity in time (i.e., the lesion formation) is the difference between the volumetric demineralisation and remineralisation rates as shown in equation 15 [adapted from Van Dijk, 1978]:

$$\frac{dE}{dt} = \left(r_{d,HAP} - r_{r,HAP}\right)\frac{M_{HAP}}{\rho_{HAP}}, \text{ with } E(0) = E_{min} \tag{15}$$

Case 2: Tooth Enamel Includes FHAP

This case tests the hypothesis that a subsurface lesion is the result of an enamel solubility gradient caused by the presence of less soluble fluoride inclusions (FHAP) near the enamel surface. To represent this situation, fluoride ions (F^-) were introduced in the model (table 2). Fluoride was considered non-reactive in saliva and dental plaque and exchangeable between all the model compartments. Only FHAP demineralisation (equation 16) is allowed in this case, without any remineralisation.

The solubility of a mixed enamel crystal containing FHAP is lower than that of HAP. It was experimentally observed that fluoride diffuses and partly replaces the hydroxyl within the first 100 μm of enamel [Moreno et al., 1974; Fejerskov and Kidd, 2008] according to the following reaction:

$$Ca_5(PO_4)_3(OH)_{1-x_F}F_{x_F} \leftrightarrows 5\,Ca^{2+} + 3\,PO_4^{3-} + (1 - x_F)HO^- + x_F F^- \tag{16}$$

The molar fraction of fluoride, $x_F = n_{F^-} / (n_{F^-} + n_{HO^-})$, decreased exponentially within 5 μm from the enamel surface from its maximum value $x_{F,max} = 0.5$ to a minimum $x_{F,min} = 0.05$ [Moreno et al., 1974] according to equation 17 (x in μm) (fig. 2):

$$x_F = x_{F,min} + (x_{F,max} - x_{F,min})\exp(x - 100) \tag{17}$$

The dependency of the mixed FHAP/HAP solubility constant, K_x, on the fraction of fluoride was measured by Moreno et al. [1974] as $K_x = \exp(8.7923\, x_F^2 - 10.2691\, x_F - 31.9308)$. These results were adjusted proportionally for the replacement of hydroxyl in enamel instead of pure HAP, $K_{S,HAP(x_F)} = K_x K_{S,HAP_{(en)}} / K_{S,HAP}$. The fraction of fluoride and the FHAP solubility constant within enamel in the first 15 μm from the tooth surface are displayed in figure 2.

We considered the same type of rate expression for the dissolution of mixed FHAP/HAP crystals (called here

HAP(x_F)) as for HAP, so that $r_{d,HAP(xF)}$ (mol HAP(x_F) m^{-3} s^{-1}) becomes:

$$r_{d,HAP(x_F)} = 0.2\, k_d \left(1 - DS_{HAP(x_F)}\right)^{m_d} \left(\sum C_{A(i)H}\right)^{n_d} a_d \tag{18}$$

$$DS_{HAP(x_F)} = \left(\frac{IP_{HAP(x_F)}}{K_{S,HAP(x_F)}}\right)^{1/9} \quad \text{and}$$
$$IP_{HAP(x_F)} = \frac{C_{Ca^{2+}}^5\, C_{Pho^{2-}}^3\, C_{F^-}^{x_F}}{C_{H^+}^{4-x_F}} K_{Pho^{2-}}^3\, K_{H_2O} \tag{19}$$

Considering that a steady fluoride content in enamel builds up over years and that the time periods simulated were relative short (hours), the contribution of FHAP remineralisation was assumed negligible and the gradient of fluoride content is stable in time. The variation of FHAP enamel porosity in time was calculated similarly to equation 15 without remineralisation:

$$\frac{dE}{dt} = r_{d,HAP(x_F)} \frac{M_{HAP}}{\rho_{HAP}}, \qquad E(0) = E_{min} \tag{20}$$

Balance Equations

The change of tooth porosity in time depends on the spatial distribution of the concentrations of several solute species (table 2). We assumed one-dimensional concentration gradients in the tooth enamel and in the dental plaque on a direction perpendicular to the tooth surface. The entire saliva volume is considered well-mixed and the concentrations are varying only in time. The one-dimensional tooth enamel domain extends from $x = 0$ (deep enamel) to $x = L_t$ (enamel-plaque interface) and the plaque is between $x = L_t$ and $x = L_t + L_p$ (the plaque-saliva interface).

Chemical species (solutes) were exchangeable between these model compartments. To calculate the solute concentrations and the amount of demineralised tooth enamel, mole and charge balances were defined on enamel, plaque and saliva domains.

Saliva

The saliva film in direct contact with the plaque has a volume V_f, and represents only a small fraction of the total saliva present in the mouth. The change in concentration of each chemical species j (table 2), $C_{f,j}(t)$, is calculated from equation 21, similar to the approach used in Ilie et al. [2012]:

$$\frac{dC_{f,j}}{dt} = \frac{Q_f}{V_f}\left(C_{s,j} - C_{f,j}\right) + \frac{A_f}{V_f} N_{p,j} + R_j \tag{21}$$

Equation 21 is based on the species exchange with the saliva bulk with a flow rate Q_f, exchange with the dental plaque of area A_f with the flux $N_{p,j}$ (diffusive flux at the plaque-saliva interface) and the net reaction rate of each component, R_j (table 1). The saliva inlet concentrations for chemical species $C_{s,j}$ are set as in a previous study [Ilie et al., 2012] (table 2), based on chemical speciation (mass-action laws) and charge balance (solution electroneutrality,

$$\sum_j z_j C_{s,j} = 0,$$

where z_j is the charge number).

For inlet concentration of glucose, repeated feeding/clearance/resting cycles having the total time of 1.5 h were imposed. In the feeding regime, $C_{s,Glu}$ quickly increased within t_{step} from $C_{Glu,min}$ to a maximum concentration $C_{s,Glu,max}$, which was maintained for the entire feeding time, t_{feed}. After feeding, clearance begins and glucose concentration decreases exponentially (equation 22) until the end of the resting period:

$$C_{s,Glu}(t) = C_{s,Glu}\left(t_{step} + t_{feed}\right) \exp\left[-\frac{Q}{V_s}\left(t - \left(t_{step} + t_{feed}\right)\right)\right] + C_{Glu,min} \tag{22}$$

The residence time ($Q/V_s = \ln(2)/t_{h,s}$) was expressed based on the halving time in the saliva bulk compartment $t_{h,s}$ [Dibdin, 1990].

Dental Plaque

In the dental plaque the solute concentrations $C_{p,j}$ change from the plaque surface to the tooth surface. Therefore, one-dimensional mole balances are set for all solutes j, as in Ilie et al. [2012] and based on Nernst-Planck equation 23 coupled with the electroneutrality condition (equation 24). Equations include net reaction rates $R_{p,j}$ and the transport by molecular diffusion ($D_{p,j}$, diffusion coefficient of a solute in the plaque at 37°C, calculated as 25% from the diffusion coefficients in water, D_j, according to Dibdin [1981]) and ion electromigration (z_j = charge number, F = Faraday's constant, R = universal gas constant and T = temperature):

$$\frac{\partial C_{p,j}}{\partial t} = D_{p,j} \frac{\partial^2 C_{p,j}}{\partial x^2} + D_{p,j} \frac{z_j F}{RT} \frac{\partial}{\partial x}\left(C_{p,j} \frac{\partial \Phi}{\partial x}\right) + R_{p,j} \tag{23}$$

$$\sum_j z_j C_{p,j} = 0 \tag{24}$$

$R_{p,j}$ is the net reaction rate of each compound, accounting for both chemical and microbial processes. The additional state variable $\Phi(x,t)$ is an electrical potential field developed due to ion transport with different diffusion rates. The initial values for all concentrations were considered equal to those in the saliva film, while the potential $\Phi(x,0) = 0$.

For the saliva-plaque interface (at $x = L_p + L_t$) the concentrations of all chemical components are equal to those in the saliva film and $\Phi = 0$ as reference value. For the plaque-tooth interface, total flux continuity is set for all the components except glucose, for which the tooth is impermeable (zero-flux condition) [Fremlin and Mathieson, 1961].

Tooth

The most important development brought by the current model compared to Ilie et al. [2012] is the explicit calculation of mineral content variation in the tooth depth. This required the representation of the tooth as another one-dimensional domain adjacent to the plaque domain. Since the focus of this study was on the initial development of subsurface lesions, only the first 100 μm in depth from the tooth surface were considered.

As in the plaque domain, the variation in time of solute concentrations (all species but glucose) is calculated by the same Nernst-Plank equations coupled with charge balance:

$$\frac{\partial C_{t,j}}{\partial t} = D_{t,j}\frac{\partial^2 C_{t,j}}{\partial x^2} + D_{t,j}\frac{z_j F}{RT}\frac{\partial}{\partial x}\left(C_{t,j}\frac{\partial \Phi}{\partial x}\right) + R_{t,j} \qquad (25)$$

$$\sum_j z_j C_{t,j} = 0 \qquad (26)$$

The net reaction rate, $R_{t,j}$, accounts only for chemical processes (acid-base equilibria and tooth (de)remineralisation) since there are no microbial species present inside the tooth. Lower enamel porosity leads to slower diffusion of any chemical species in the tooth domain $D_{t,j} = D_j\, E$ in respect to diffusivities in water, D_j, from table 2 [Ten Cate, 1979]. The enamel porosity is variable in time and over the tooth depth, $E(x,t)$, and it is calculated differently, function of the tested hypothesis, with equation 15 (case 1) or equation 20 (case 2). The boundary conditions were: flux continuity at the plaque-tooth interface and zero-flux/electrical insulation at the deep enamel boundary ($x = 0$). Initial concentrations of chemical components in the tooth are equal to those in the plaque and the initial porosity is E_{min} (i.e., healthy enamel).

Model Solution

The model equations were implemented in COMSOL Multiphysics software (COMSOL 4.1, COMSOL Inc., Burlington, Mass., USA, www.comsol.com), which allows a very flexible and well-structured model construction. COMSOL solves the resulting system of ordinary differential, partial differential and algebraic equations by finite element methods. The plaque domain was discretized on a mesh of 100 elements with finer mesh size next to both the saliva and enamel boundaries. The mesh in the tooth domain contained also 100 elements of size and finer meshing at the enamel surface, where the concentration gradients can become very steep.

First, the mole and charge balances in plaque and enamel (equations 23–26) were solved towards the steady state solution, which represents a situation of resting plaque in contact with constant composition saliva. Second, the steady state solution was used as initial condition for the time-dependent simulations performed during 80 sequential feeding/clearance/resting cycles of 1.5 h each. The time-dependent simulations included the complete model equations in saliva (equation 21), plaque (equations 23, 24) and tooth (equations 25, 26 and 15 or 20), with the associated boundary conditions and constitutive (rate) equations.

Results

The numerical model described in this study is aiming to offer a better understanding of the mechanisms leading to a tooth subsurface lesion under the influence of acids produced in dental plaque. Two cases were chosen in order to distinguish whether the lesion could be caused solely by an alternation of demineralisation/remineralisation processes (i.e., originating from the same thermodynamic force) or by a fluoride gradient (and implicitly solubility gradient). In case 1, tooth enamel consists of HAP with demineralisation and remineralisation, and in case 2 tooth enamel contains a mixture of HAP and FHAP with only demineralisation occurring. For each case we analysed (1) the influence of glucose pulses on the pH and the total amount of demineralised enamel at tooth surface in time, (2) the pH profile, concentration of calcium ions and total phosphate species over the plaque depth as well as demineralisation and remineralisation rates within the enamel at a certain time, and (3) the evolution of porosity profiles inside the enamel.

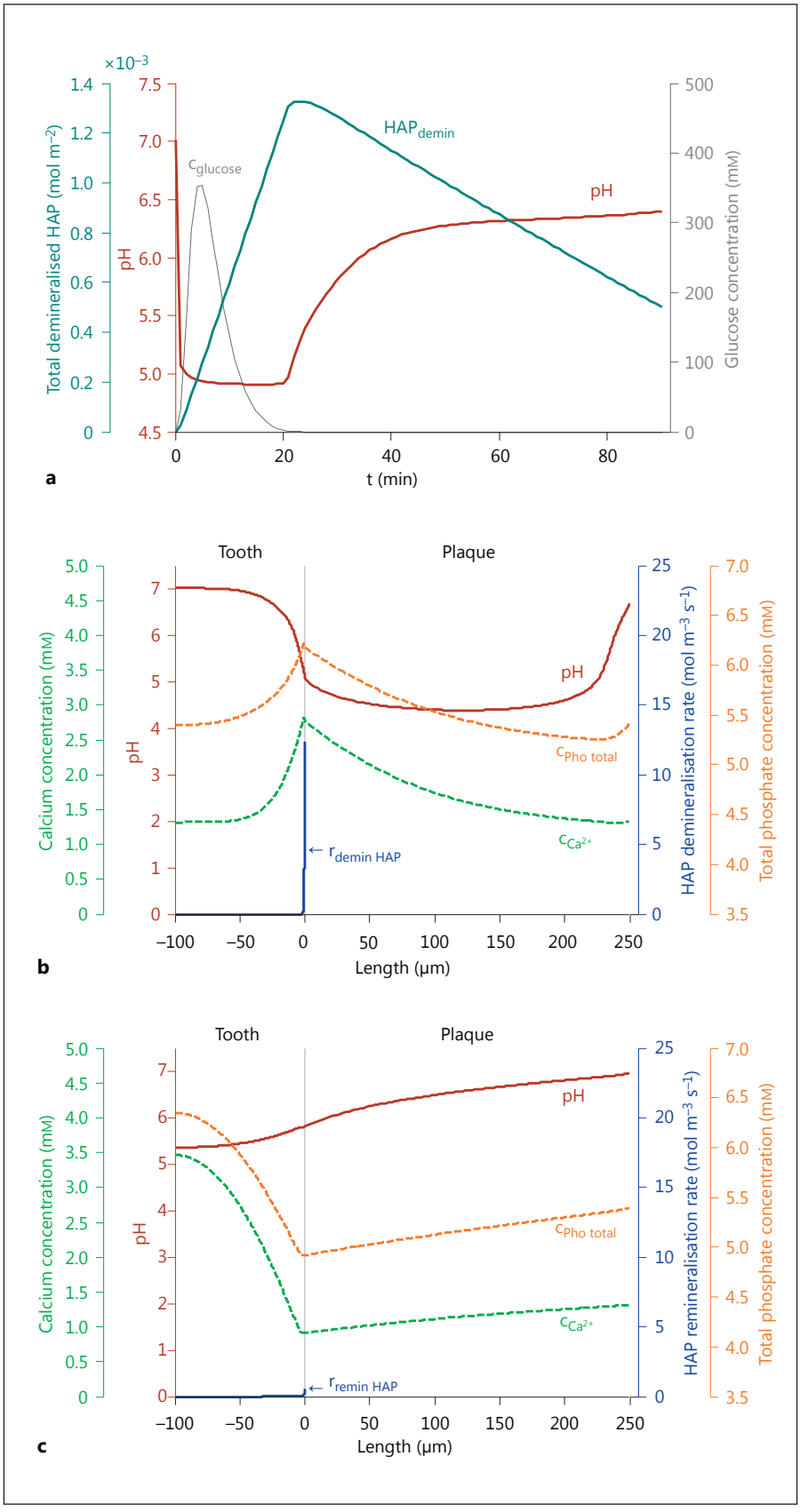

Color version available online

Fig. 3. Calculated concentration profiles for case 1, when the tooth enamel contains only HAP. **a** pH, glucose concentration and total amount of demineralised HAP at the tooth surface during one feeding/resting cycle. **b** Concentrations of calcium and total phosphate, pH and rate of HAP demineralisation along the dental plaque and in the tooth enamel after 1 min from the beginning of the first feeding/resting cycle. The grey dotted line represents the plaque-tooth boundary. **c** Concentrations of calcium and total phosphate, pH and rate of HAP remineralisation profile along the dental plaque and in the tooth enamel after 30 min from the beginning of the first feeding/resting cycle.

Case 1: Tooth Enamel Consisting of HAP

Concentration Profiles

Feeding/Resting Cycle. The glucose concentration at the tooth surface and its influence on the pH profile at the tooth surface (Stephan curve) and subsequently on the amount of HAP lost in time are shown in figure 3a. Moments after the concentration of glucose in saliva has increased, the pH at the tooth surface sharply decreases below the critical value for demineralisation ($pH_{critical} = 5.5$). In these conditions, the plaque fluid at the tooth surface becomes undersaturated with respect to HAP ($DS_{HAP} < 1$) and the tooth enamel starts to demineralise. As long as there is glucose in the plaque, the pH stays acidic and an increasing amount of HAP is lost. After approximately 20 min from the beginning of the cycle, when the glucose is cleared from the saliva and dental plaque, the pH starts to restore towards the steady state value. As soon as the pH rises above 5.5, the amount of HAP lost decreases, meaning that remineralisation is now active. While remineralisation is active (i.e., $E > 0.01$ and $DS_{HAP} > 1$), the pH cannot restore to the steady state value of 7 due to the continuous consumption of hydroxyl ions during this process (equation 4). Restoration to steady state values in tooth and plaque can occur only when the tooth is completely remineralised (i.e., $E = E_{min} = 0.01$). In the current case, the tooth is not fully remineralised at the end of the 90 min cycle, and there is a net loss of approximately 5×10^{-4} mol HAP m^{-2} per cycle (fig. 3a). This corresponds to 10^{-4} mg Ca mm^{-2} lost per cycle, an amount in the same order of magnitude with the experimental observations of Margolis and Moreno [1992] and with the results of our previous model [Ilie et al., 2012]. The net amount of lost HAP per feeding/resting cycle depends thus on the length of the remineralisation stage.

Demineralisation Phase. An example of concentration profiles along the dental plaque and tooth domains for the ions influencing DS_{HAP} (i.e., calcium, total phosphates and protons/pH), after 1 min in the feeding period (i.e., during the acid attack and maximum demineralisation rate) is presented in figure 3b. At this time, the maxima of total phosphate and calcium concentrations are close to the enamel surface, where these components are released by HAP demineralisation, and diffuse towards the plaque surface (therefore the linear concentration profile, showing also that a quasi-steady state was reached in the plaque). These species diffuse also inside the tooth, but much slower, therefore the concentration profiles are curved and far from steady state. The HAP demineralisation in which these species are produced occurs only in a very narrow region in the tooth where $pH < pH_{critical}$. In the plaque depth, the pH decreases from nearly neutral in saliva to almost 5 at the tooth surface. This decrease is caused by the microbial production of organic acids. Within the tooth enamel the pH increases to neutral values far from the tooth surface due to the slower diffusion of protons inside the tooth compared to the plaque. The proton consumption in demineralisation leads also to a small pH increase in the plaque depth.

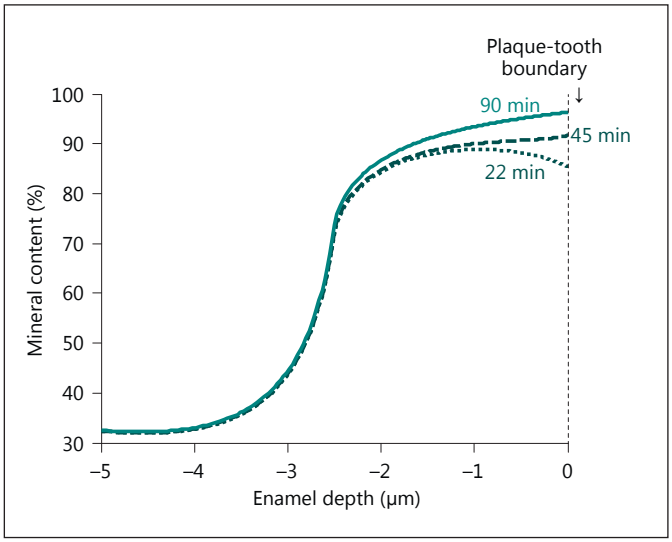

Fig. 4. Calculated mineral content profiles in the tooth enamel at different stages during the 80th feeding/resting cycle. 22 min: end of demineralisation stage; 45 min: during remineralisation; 90 min: at the end of the remineralisation (resting) period.

Remineralisation Phase. After 30 min from the beginning of the feeding/resting cycle, during the remineralisation stage, the calcium and phosphate are consumed in the tooth, therefore their fluxes are reversed compared to the demineralisation stage (fig. 3c). At this time, the maximum concentrations are at the saliva-plaque boundary and the minimum at the tooth surface where the ions are consumed. Although the pH is above the critical value along the entire tooth domain, the remineralisation reaction takes place only in a narrow region at the very surface of the tooth. This means that during the previous demineralisation stage, only a narrow region of HAP enamel was demineralised, leading to porosity values higher than E_{min}. The maximum calculated rate of remineralisation is approximately ten times smaller than the maximum rate of demineralisation and is in the same range as the rates experimentally observed by de Rooij and Nancollas [1984] and White et al. [1988].

Table 3. Sensitivity analysis results

Parameter name/ Parameter value	Diffusion inside the tooth ($D_{t,j}$) (f_{min} = 0.2)		Remineralisation rate constant (k_m) (f_{min} = 0.2; f_{max} = 5)		Length of feeding/resting cycle (t_{cycle}) (f_{min} = 0.5; f_{max} = 2)	
	lost HAP[a], mmol HAP m^{-2}	min. HAP content[b], %	lost HAP[a], mmol HAP m^{-2}	min. HAP content[b], %	lost HAP[a], mmol HAP m^{-2}	min. HAP content[b], %
f_{min} × standard value	12.6	40	14.9	69	29	36
Standard value	14.6	64	14.6	64	14.6	64
f_{max} × standard value	–	–	14.4	60	1.5	96

[a] Amount of HAP lost at the end of all the 25 feeding/resting cycles. [b] Minimum content of HAP at the end of the 25th feeding/resting cycle.

Mineral Profiles during One Cycle. The mineral content along the first 5 μm from the tooth surface at different stages after the beginning of the feeding/resting cycle is represented in figure 4 for the 80th cycle. The model clearly demonstrates how a subsurface lesion is formed after many feeding/resting cycles only by alternating phases of demineralisation and remineralisation. The most chemically active part of the tooth appears to be near its surface: the HAP content during demineralisation (22 min) is 15% lower than the content of the same region at the end of the cycle (90 min). The current model suggests that a pre-existing gradient (such as in the enamel solubility constant [Van Dijk et al., 1979; Arends and Christoffersen, 1986], or demineralisation/remineralisation reaction rate constants [Ten Cate, 1979], or fluoride distribution [Wang et al., 1996]) is not required in order to develop a subsurface lesion when remineralisation is present. The remineralisation rate is highest at the tooth surface. If the remineralisation period is long enough, the entire lesion can remineralise. However, for short recovery times (as it is the case for frequent sugar consumption) the lesion can remineralise only superficially, while higher porosity builds up in the lesion depth. Therefore, the porosity of the surface layer will remain within certain limits (1–15% in the current model) while the porosity in the subsurface area will slowly increase with each demineralisation-remineralisation cycle (for example, up to 75% as shown in movie 1 in the online supplementary material; for all online suppl. material, see www.karger.com/doi/10.1159/000354123).

Sensitivity Analysis

Important factors to be considered when discussing the development of a mineral surface layer via remineralisation are (1) the diffusion coefficient inside the tooth, (2) the HAP remineralisation rate and (3) length of the remineralisation period (resting time). To study their influence, a sensitivity analysis was performed. For these parameters, simulations were run for 25 feeding/resting cycles, with the base value and with increased/decreased parameter values (table 3).

Diffusion inside the Tooth. A subsurface lesion was obtained for each tested value of the diffusion coefficients in the tooth (fig. 5a). However, it appears that the faster the diffusion, the less pronounced (higher mineral content) but wider and deeper within the enamel the lesion forms. Indeed, faster diffusion creates a more evenly distributed concentration profile of ions (and consequently DS_{HAP}) within the enamel, and the demineralisation reaction is active over an extended depth. Although the lesion appears to be less severe for faster diffusion, the total amount of mineral lost is still the highest, with ~10% more HAP lost compared to the slower diffusion case (table 3). Therefore, the effective diffusion of chemical species within the tooth has a significant influence on the shape of the lesion and on the time when the porosity becomes large enough to make the lesion clinically observable.

Remineralisation Rate. The kinetics of remineralisation may influence the mineral profile, therefore the remineralisation rate constant (k_m) was also varied (fig. 5b). The simulated lesions had very similar mineral profiles, with only 1% more HAP lost for the highest k_m value compared with the standard case (table 3). For slower remineralisation rate, the surface layer remains porous for extended periods of time, thus with increased effective diffusivity. This allows ions to penetrate deeper inside the tooth and to better restore the demineralised enamel. In conclusion, small variations in remineralisation rate may not influence significantly the formation of a subsurface lesion, but only the 'quality' of the surface layer formed.

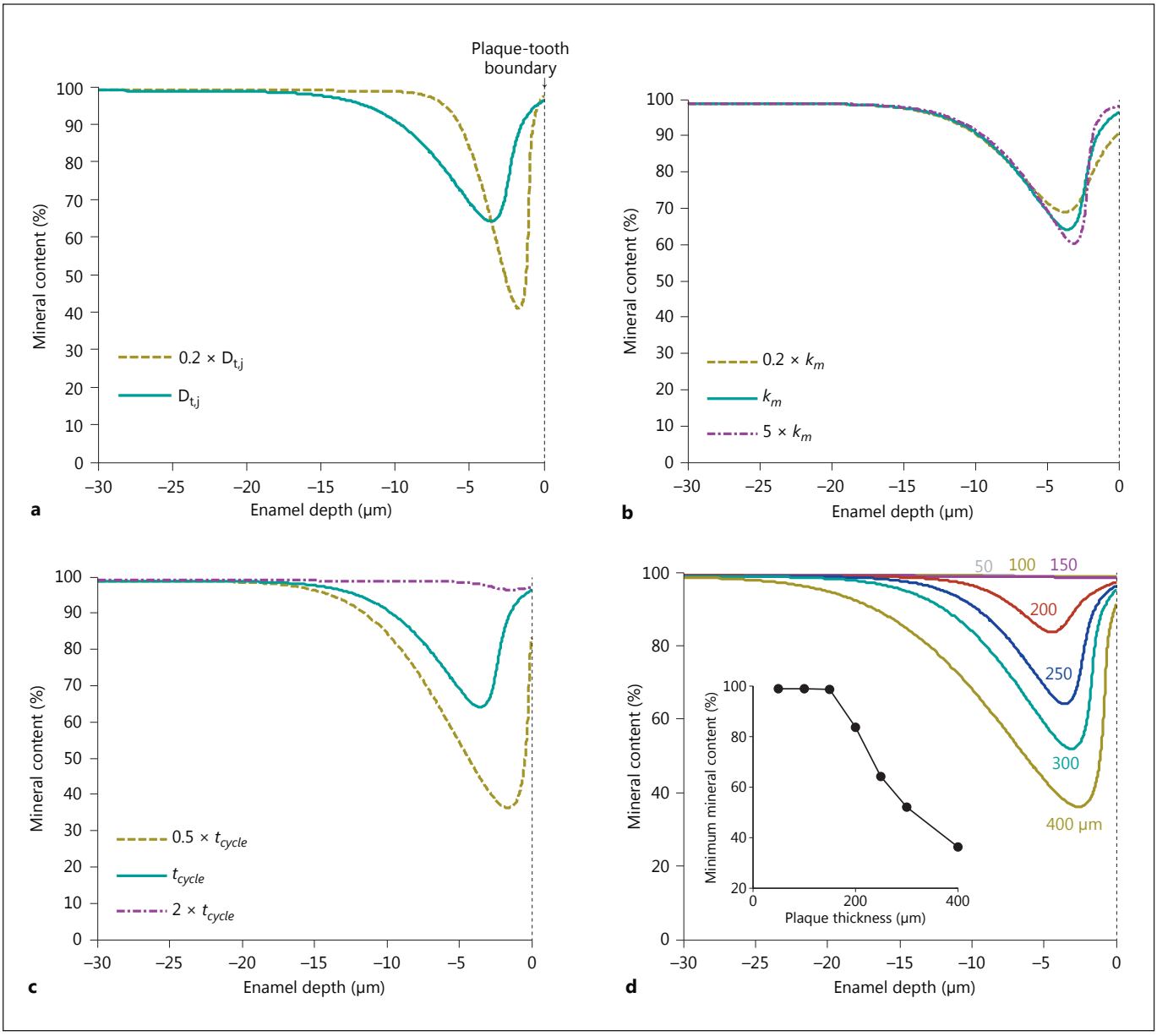

Color version available online

Fig. 5. Mineral content in the enamel at the end of the 25th feeding/resting cycle, with various parameter values for the demineralisation-remineralisation model (case 1): **a** effective diffusion coefficient in the enamel; **b** remineralisation rate constant; **c** length of the feeding/resting cycle; **d** plaque thickness between 50 and 400 μm. The insert shows the minimum mineral content reached after 25 cycles as a function of the plaque thickness.

Length of the Remineralisation Phase. The highest impact on lesion formation proved to be the length of the remineralisation period. This is a behavioural factor, determined by the eating habits of the individual because caries formation is mainly associated with frequent sugar intake and therefore short remineralisation time. For longer remineralisation times (t_{cycle} = 180 min) there is no lesion formed at the end of the 25th feeding/resting cycle (fig. 5c). This shows that given enough time, the lesion formed after an acid attack could be fully remineralised. However, for a shorter remineralisation time (t_{cycle} = 30 min), the lesion is formed directly at the tooth surface and no surface layer is present, giving the highest amount of HAP lost from all the cases studied (table 3). The res-

Caries Res 2014;48:73–89
DOI: 10.1159/000354123

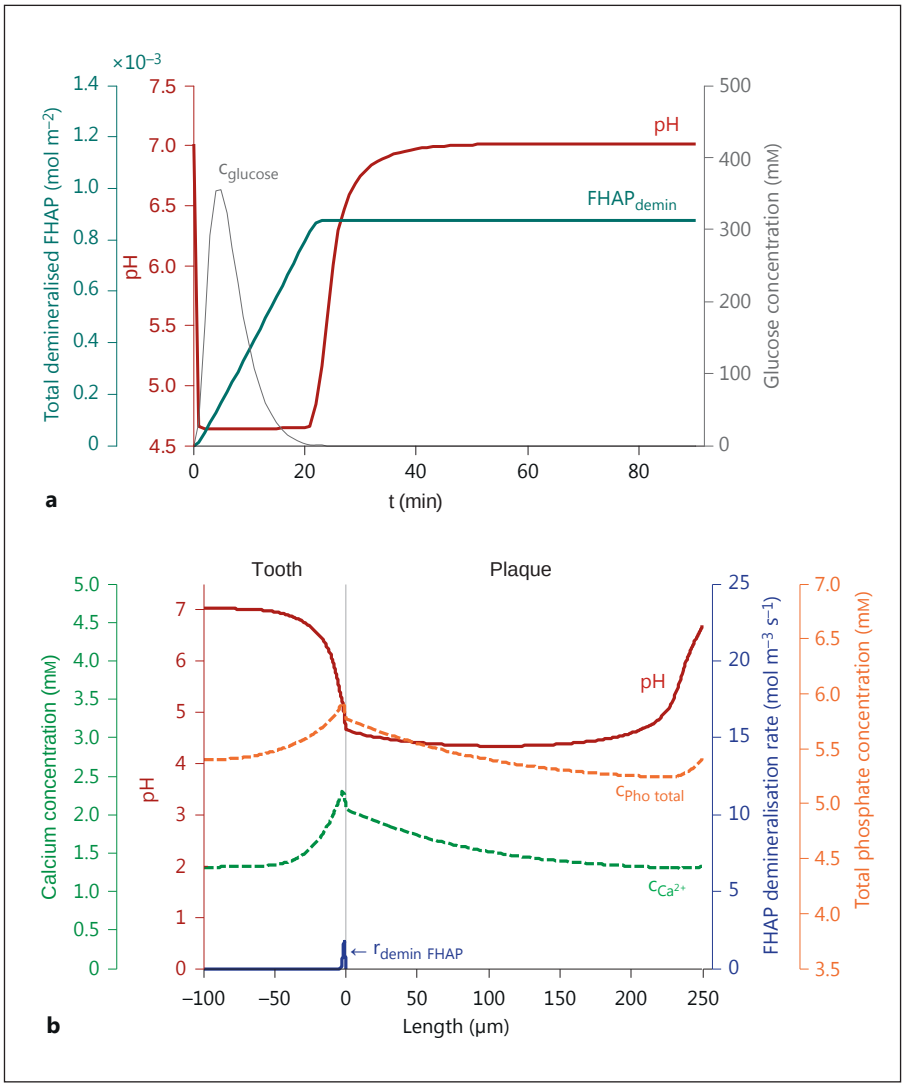

Color version available online

Fig. 6. Calculated concentration profiles for case 2, when the tooth enamel contains a fluoride distribution. **a** pH, glucose concentration and total amount of demineralised FHAP at the tooth surface during one feeding/resting cycle. **b** Concentrations of calcium and total phosphate, pH and rate of FHAP demineralisation along the dental plaque and in the tooth enamel after 1 min from the beginning of the first feeding/resting cycle. The grey dotted line represents the plaque-tooth boundary.

toration period is therefore very important and the numerical simulations support the widespread observation that often consumption of sugars is a key factor in caries formation.

Plaque Thickness. Interestingly, the model of enamel demineralisation and remineralisation allows the identification of a minimum plaque thickness that can induce a lesion. With the current model parameters (case 1), for plaque thickness L_p <150 µm there was no significant mineral loss (fig. 5d). Above 150 µm, the thicker the plaque the more extensive enamel lesions developed. It should be noted that the model only indicates the existence of a critical plaque thickness needed for the development of an incipient caries lesion. The value of this critical thickness is subjected to many parameters, such as the length of remineralisation phase, plaque composition and activity, salivary flow and composition, etc. Showing that caries onset can be prevented by reducing, though not completely eliminating, the plaque would be relevant to understanding appropriate oral hygiene protocols.

Case 2: Tooth Enamel Includes FHAP

This case tested in what extent the subsurface lesion is the result of an increased enamel resistance to acid attacks due to the presence of less soluble fluoride inclusions near the enamel surface. The glucose concentration at the tooth surface, the pH at the tooth surface and the total

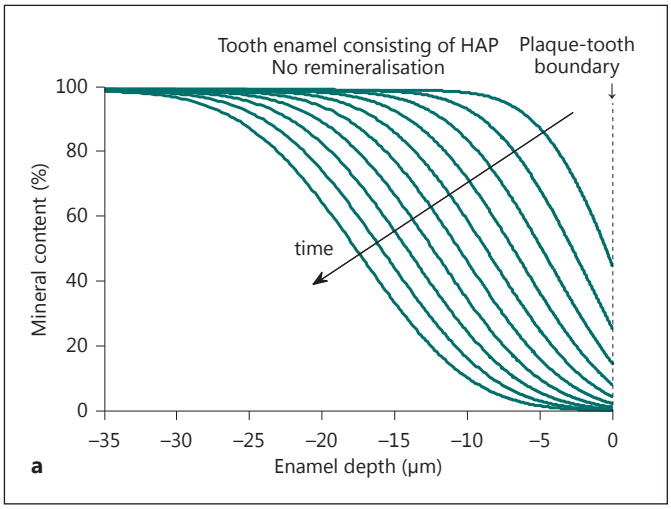

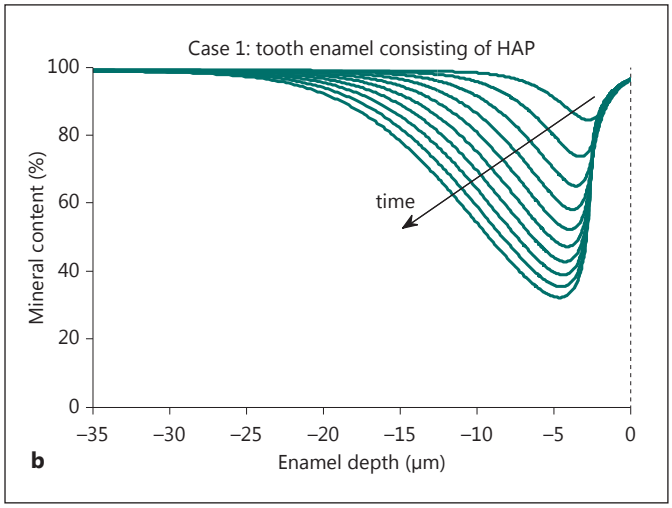

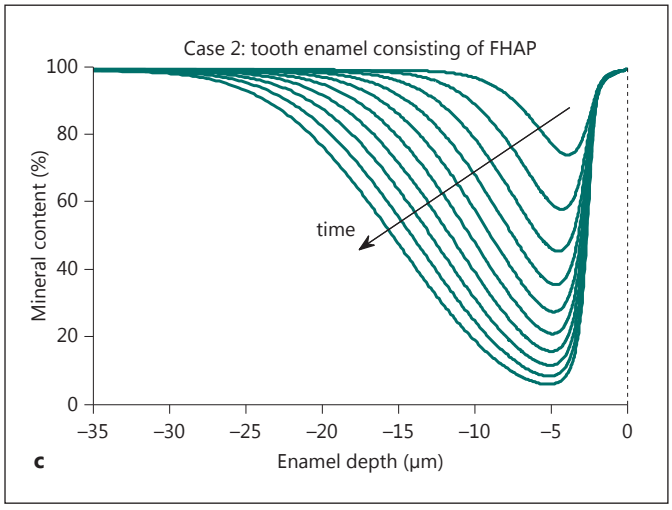

Color version available online

Fig. 7. Calculated mineral content profiles (progression of caries lesion) inside the tooth enamel at the end of each 8th feeding/resting cycle. The plaque-tooth boundary is represented at depth zero. **a** Only demineralisation without any remineralisation. **b** Demineralisation and remineralisation of HAP (case 1). **c** Demineralisation of FHAP/HAP (case 2). Animations of calculated mineral content evolution are presented in online supplementary movies 1 and 2.

amount of demineralised FHAP during one cycle in this case are displayed in figure 6a. The same correlation is noticed between the glucose pulse, the sudden pH drop and the increasing amount of demineralised FHAP. Since there is no remineralisation process in this case, the amount of FHAP remains constant once the demineralisation has stopped. The lower solubility of FHAP compared to HAP is reflected in the smaller amount of demineralised FHAP compared with case 1. The minimum pH value is lower than the one obtained for the HAP case, due to the lower buffer capacity at lower concentrations of phosphate released during demineralisation.

Qualitatively, the profiles of the total phosphate species and calcium ion concentrations in this case (fig. 6b) resemble those for case 1 (fig. 3b), one minute after the beginning of the feeding/resting cycle. The maximum rate of FHAP demineralisation was in this case 6 times lower than the HAP demineralisation rate and it led to lower concentrations of calcium and total phosphate species in the plaque. As expected, the first few micrometres of enamel do not dissolve due to the fluoride presence, but there is still mineral loss under this surface layer. This was also assumed in the model of Wang et al. [1996] on fluoride adsorption in enamel and experimentally observed by Chu et al. [1989]. It remains questionable whether the surface layer is completely inert in vivo during lesion development. Experimental data are available on the development of subsurface lesions in environments both with and without fluoride [Nancollas, 1983; Theuns et al., 1984; Margolis et al., 1999]. Although fluoride presence may not be the sole reason for the development of a subsurface lesion, the model shows how fluoride distribution alone can lead to subsurface lesions comparable with the experimental observations.

Comparison of the Lesions

Formation of surface layers in time was compared for the studied cases: (1) HAP without remineralization (fig. 7a); (2) HAP by alternating demineralisation/remineralisation periods (fig. 7b); (3) HAP/FHAP by imposing a fluoride distribution over the tooth domain (fig. 7c). As expected, there was no surface layer present and the carious lesion formed at the tooth surface without remineralisation because there was no restoring process to balance the demineralisation damage (fig. 7a). After each demineralisation cycle, the mineral content near the surface would decrease, and the simulated lesion extended in the enamel depth at a quasi-constant rate, reaching approximately 30 μm after 80 feeding/resting cycles.

When remineralisation was active (case 1), at the end of the 80th cycle the minimum mineral content reached 30% within the first 5 μm of tooth enamel, with a distinct surface layer formed at the tooth-plaque interface (fig. 7b). The decrease in mineral content near the surface layer to the minimum value in the body of the lesion was very abrupt, while the damage caused deeper within the tooth was more gradual. This can be explained by the faster mineral regeneration at the tooth surface than in the deeper layers, leading to a fully regenerated surface. As the number of cycles (i.e., acid attacks) increases, a more pronounced subsurface lesion developed inside the tooth (see movie 1 in the online suppl. material). The obtained profile is very similar to the mineral content profiles determined experimentally by Margolis et al. [1999].

In case the tooth enamel contained FHAP crystals but no remineralisation occurred (case 2), the obtained profiles resembled qualitatively those obtained for HAP with demineralisation/remineralisation (fig. 7c). The most notable differences were however the almost complete mineral dissolution in the subsurface lesion after 80 cycles and a faster progression of the lesion in the tooth depth (see movie 2 in online suppl. material). However, these late stages of lesion development are less probable to occur in vivo. There is a limit to the mineral content in the subsurface lesion after which the surface layer brakes during mastication and cavitation exposes the body of the lesion.

Discussion

This study developed a numerical model that couples tooth demineralisation and remineralisation with metabolic processes in the dental plaque. It was found that a subsurface lesion can be achieved using the same thermodynamic driving force (degree of saturation leading to demineralisation or remineralisation) and without any preimposed gradients.

There is a debate in dentistry regarding the importance of the remineralisation phenomena for the formation of a surface layer. The model results are discussed here in the context of early stage carious lesions, the so-called 'white spots'. One point of view is that what appears to be a restored surface is partly explained in terms of wear and polishing [Fejerskov and Kidd, 2008]. Although it is possible that polishing plays a role in the aspect of a restored tooth surface, this does not exclude the existence of remineralisation. Furthermore, there is experimental evidence that the surface layer has more than just the aspect of a restored surface; it also has a mineral content close to that of healthy enamel [Silverstone, 1977; Fejerskov and Kidd, 2008].

Another argument is that inhibitor molecules present in saliva (e.g., statherin) prevent in vivo precipitation at crystal surface by blocking crystallization nuclei [Santos et al., 2008]. However, the presence of these inhibitors does not imply that the process of remineralisation is entirely blocked, but only indicates that remineralisation in vivo would occur more slowly (fig. 5b). It was also argued that the very fast uptake of calcium and phosphate by the HAP makes the pore liquid in the deep layers of lesion only marginally saturated [Larsen and Fejerskov, 1989], thus remineralisation can only be very slow.

A widespread theory is also that since the surface enamel remineralises faster, an area of lower porosity at the tooth surface is created. This surface layer acts as a diffusion barrier that restricts further access of HAP constituent ions in the deeper layers of the lesion and stops the remineralisation [Silverstone, 1977; Larsen and Fejerskov, 1989; Robinson et al., 2000]. Although it is true that such a barrier is formed, this can only delay the diffusion of the ions inside the lesion (fig. 5a). If the remineralisation time is long enough, the deep layers of the lesion can still be restored (fig. 5c).

According to Arends and Christoffersen [1986], the experimental observation that a surface layer once formed has a nearly constant thickness supports the idea that the surface layer forms because of a solubility gradient along the enamel depth. With the model described in this study, a surface layer of nearly constant thickness was obtained in both cases.

The surface layer can develop only by alternating periods of demineralisation (corresponding to sugar consumption) and remineralisation (corresponding to rest-

ing between meals) in tooth enamel with uniform mineral composition. Sensitivity analysis showed that surface layer formation is strongly dependent on the length of remineralisation and demineralisation cycles and on plaque thickness. This confirms once more that the behavioural aspect of caries formation (i.e., length of resting phase, frequency of sugar consumption, tooth brushing) is very important. It was also shown how the presence of a fluoride gradient leads to subsurface lesions. The calculated profiles of mineral content in enamel are similar to those observed experimentally in vitro and in vivo [Margolis et al., 1999]. Most probably, both mechanisms studied in the present paper interact in vivo in the process of caries development.

Acknowledgement

This work was financially supported by the Netherlands Organization for Scientific Research (NWO, VIDI grant 864.06.003).

References

Arends J, Christoffersen J: The nature of early caries lesions in enamel. J Dent Res 1986;65:2–11.

Atkins P, De Paula J: Physical Chemistry, ed 9. Oxford, W.H. Freeman, 2009.

Borgström MK, Edwardsson S, Sullivan Å, Svensäter G: Dental plaque mass and acid production activity of the microbiota on teeth. Eur J Oral Sci 2000;108:412–417.

Chu JS, Fox JL, Higuchi WI: Quantitative study of fluoride transport during subsurface dissolution of dental enamel. J Dent Res 1989;68:32–41.

Dawes C, Dibdin GH: A theoretical analysis of the effects of plaque thickness and initial salivary sucrose concentration on diffusion of sucrose into dental plaque and its conversion to acid during salivary clearance. J Dent Res 1986;65:89–94.

De Rooij JF, Nancollas GH: The formation and remineralization of artificial white spot lesions – a constant composition approach. J Dent Res 1984;63:864–867.

Dibdin GH: Diffusion of sugars and carboxylic acids through human dental plaque in vitro. Arch Oral Biol 1981;26:515–523.

Dibdin GH: Effect on a cariogenic challenge of saliva/plaque exchange via a thin salivary film studied by mathematical modelling. Caries Res 1990;24:231–238.

Dirksen TR, Little MF, Bibby BG, Crump SL: The pH of carious cavities. I. The effect of glucose and phosphate buffer on cavity pH. Arch Oral Biol 1962;7:49–57.

Fejerskov O, Kidd E: Dental Caries: The Disease and Its Clinical Management, ed 2. Chichester, Blackwell Munksgaard, 2008.

Fremlin JH, Mathieson J: A microchromatographic study of the penetration of enamel by C14-labelled glucose. Arch Oral Biol 1961;4:92–96.

Gray JA, Francis MD: Physical chemistry of enamel dissolution; in Sognnaes RF (ed): Destruction of Hard Tissues. Publication No 75. Washington, American Association for the Advancement of Science, 1963, pp 213–260.

Hamilton IR, St Martin EJ: Evidence for the involvement of proton motive force in the transport of glucose by a mutant of *Streptococcus mutans* strain DR0001 defective in glucose-phosphoenolpyruvate phosphotransferase activity. Infect Immun 1982;36:567–575.

Hicks J, Garcia-Godoy F, Flaitz C: Biological factors in dental caries enamel structure and the caries process in the dynamic process of demineralization and remineralization (part 2). J Clin Pediatr Dent 2004;28:119–124.

Hollander F, Saper E: The apparent radiopaque surface layer of the enamel. Dent Cosmos 1935;77:1187–1197.

Holly FJ, Gray JA: Mechanism for incipient carious lesion growth utilizing a physical model based on diffusion concepts. Arch Oral Biol 1968;13:319–334.

Ilie O, van Loosdrecht MC, Picioreanu C: Mathematical modelling of tooth demineralisation and pH profiles in dental plaque. J Theor Biol 2012;309:159–175.

Koutsoukos P, Amjad Z, Tomson MB, Nancollas GH: Crystallization of calcium phosphates. A constant composition study. J Am Chem Soc 1980;102:1553–1557.

Langdon DJ, Elliott JC, Fearnhead RW: Microradiographic observation of acidic surface decalcification in synthetic apatite aggregates. Caries Res 1980;14:359–366.

Larsen MJ, Fejerskov O: Chemical and structural challenges in remineralisation of dental enamel lesions. Scand J Dent Res 1989;97:285–296.

Loesche WJ: Role of *Streptococcus mutans* in human dental decay. Microbiol Rev 1986;50:353–380.

Margolis HC, Moreno EC: Kinetic and thermodynamic aspects of enamel demineralization. Caries Res 1985;19:22–35.

Margolis HC, Moreno EC: Kinetics of hydroxyapatite dissolution in acetic, lactic and phosphoric acid solutions. Calcif Tissue Int 1992;50:137–143.

Margolis HC, Zhang YP, Lee CY, Kent RL, Moreno JR, Moreno EC: Kinetics of enamel demineralisation in vitro. J Dent Res 1999;78:1326–1335.

Marsh PD, Martin MV, Lewis MAO, Williams DW: Oral Microbiology, ed 5. London, Churchill Livingstone Elsevier, 2009.

Moreno EC, Kresak M, Zahradnik RT: Fluoridated hydroxyapatite solubility and caries formation. Nature 1974;247:64–65.

Morgenroth E, Eberl H, van Loosdrecht MCM: Evaluating 3-D and 1-D mathematical models for mass transport in heterogeneous biofilms. Water Sci Technol 2000;41:347–356.

Nancollas GH: Kinetics of demineralisation and remineralisation; in Leach SA, Edgar WM (eds): Demineralization and Remineralization of the Teeth. Oxford, IRL Press, 1983, pp 113–128.

Robinson C, Shore RC, Brookes SJ, Strafford S, Wood SR, Kirkham J: The chemistry of enamel caries. Crit Rev Oral Biol Med 2000;11:481–495.

Santos O, Kosoric J, Hector MP, Anderson P, Lindh L: Adsorption behavior of statherin and a statherin peptide onto hydroxyapatite and silica surfaces by in situ ellipsometry. J Colloid Interface Sci 2008;318:175–182.

Silverstone LM: Remineralization phenomena. Caries Res 1977;11(suppl 1):59–84.

Ten Cate JM: Remineralization of Enamel Lesion. A Study of the Physico-Chemical Mechanism. Dissertation, University of Groningen, The Netherlands, 1979.

Ten Cate JM: A model for enamel lesion remineralisation; in Leach SA, Edgar WM (eds): Demineralization and Remineralization of the Teeth. Oxford, IRL Press, 1983, pp 129–144.

Ten Cate JM: Remineralization of deep enamel dentine caries lesions. Aust Dent J 2008;53:281–285.

Theuns HM, van Dijk JWE, Driessens FCM, Groeneveld A: The surface layer during artificial carious lesion formation. Caries Res 1984;18:97–102.

Van Beelen P, van der Hoeven JS, De Jong MH, Hoogendoorn H: The effect of oxygen on the growth and acid production of *Streptococcus mutans* and *Streptococcus sanguis*. FEMS Microbiol Lett 1986;38:25–30.

Van der Hoeven JS, De Jong MH, Camp PJM, van den Kieboom CWA: Competition between oral *Streptococcus* species in the chemostat under alternating conditions of glucose limitation and excess. FEMS Microbiol Lett 1985; 31:373–379.

Van der Hoeven JS, Gottschal JC: Growth of mixed cultures of *Actinomyces viscosus* and *Streptococcus mutans* under dual limitation of glucose and oxygen. FEMS Microbiol Lett 1989;62:275–284.

Van der Hoeven JS, van den Kieboom CW, Camp PJ: Utilization of mucin by oral *Streptococcus* species. Antonie van Leeuwenhoek 1990;57: 165–172.

Van Dijk JWE: The Electrochemistry of Dental Enamel and Caries. Dissertation, University of Nijmegen, The Netherlands, 1978.

Van Dijk JWE, Borggreven JMPM, Driessens FCM: Chemical and mathematical simulations of caries. Caries Res 1979;13:169–180.

Vanýsek P: Handbook of Chemistry and Physics, ed 82. Boca Raton, CRC Press LLC, 2001, pp 5–95, 6–194.

Wang Z, Fox JL, Baig AA, Otsuka M, Higuchi WI: Calculation of intercrystalline solution composition during in vitro subsurface lesion formation in dental minerals. J Pharm Sci 1996; 85:117–128.

White DJ, Chen WC, Nancollas GH: Kinetic and physical aspects of enamel remineralisation – a constant composition study. Caries Res 1988;22:11–19.

Wood SR, Kirkham J, Marsh PD, Shore RC, Nattress B, Robinson C: Architecture of intact natural human plaque biofilms studied by confocal laser scanning microscopy. J Dent Res 2000;79:21–27.

Zimmerman SO: A mathematical theory of enamel solubility and the onset of dental caries: I. The kinetics of dissolution of powdered enamel in acid buffer. Bull Math Biophys 1966a;28:417–432.

Zimmerman SO: A mathematical theory of enamel solubility and the onset of dental caries: II. Some solubility equilibrium considerations of hydroxyapatite. Bull Math Biophys 1966b;28:433–441.

Zimmerman SO: A mathematical theory of enamel solubility and the onset of dental caries: III. Development and computer simulation of a model of caries formation. Bull Math Biophys 1966c;28:443–464.